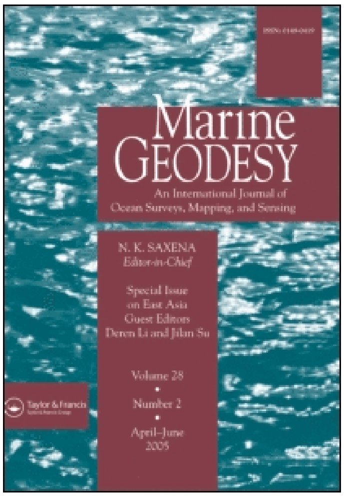

Marine Geodesy
Publication details, including instructions for authors and subscription information:
http://www.informaworld.com/smpp/title~content=t713657895

Comparison of Sea Surface Heights Derived from Satellite Altimetry and from Ocean Bottom Pressure Gauges: The SW Pacific MOTEVAS Project

S. Calmant[a]; K. Cheng[b]; G. Jan[c]; C. Kuo[d]; C. Shum[d]; Y. Yi[d]; V. Ballu[e]; M. -N. Bouin[a]
[a] Laboratoire d'Etudes en Geophysique et Océanographie Spatiales Observatoire Midi-Pyrénées Toulouse, France, [b] Laboratory for Space Geodesy and Remote Sensing Research, Columbus, Ohio, USA [c] Noveltis Parc Technologique du Canal Ramonville, France, [d] Laboratory for Space Geodesy and Remote Sensing Research Columbus, Ohio, USA, [e] Laboratoire de Gravimétrie et Géodynamique Institut de Physique du Globe Paris, France,

To cite this Article Calmant, S. , Cheng, K. , Jan, G. , Kuo, C. , Shum, C. , Yi, Y. , Ballu, V. and Bouin, M. -N.(2004) 'Comparison of Sea Surface Heights Derived from Satellite Altimetry and from Ocean Bottom Pressure Gauges: The SW Pacific MOTEVAS Project', Marine Geodesy, 27: 3, 597 — 613

To link to this Article: DOI: 10.1080/01490410490883379

URL: http://dx.doi.org/10.1080/01490410490883379

Marine Geodesy, 27: 597–613, 2004

ISSN: 0149-0419 print / 1521-060X online
DOI: 10.1080/01490410490883379

Comparison of Sea Surface Heights Derived from Satellite Altimetry and from Ocean Bottom Pressure Gauges: The SW Pacific MOTEVAS Project

S. CALMANT

Laboratoire d'Etudes en Geophysique et Océanographie Spatiales
Observatoire Midi-Pyrénées
Toulouse, France

K. CHENG

Laboratory for Space Geodesy and Remote Sensing Research
Columbus, Ohio, USA

G. JAN

Noveltis
Parc Technologique du Canal
Ramonville, France

C. KUO
C. SHUM
Y. YI

Laboratory for Space Geodesy and Remote Sensing Research
Columbus, Ohio, USA

V. BALLU

Laboratoire de Gravimétrie et Géodynamique
Institut de Physique du Globe
Paris, France

Received 14 May 2004; accepted 16 June 2004.

The authors are indebted to the crew of R/V *Alis*, the divers of the Centre IRD at Nouméa, New Caledonia, and J. M. Bore who headed the cruises and supervised the installation and maintenance of the bottom pressure gauges. The Ohio State University team acknowledges support of the research from NASA's Interdisciplinary Science (IDS) program and the Ohio Sea Grant program. The authors acknowledge D. Chambers of the University of Texas and an anonymous reviewer for their constructive comments.

Address correspondence to S. Calmant, Laboratoire d'Etudes en Geophysique et Océanographie Spatiales, Observatoire Midi-Pyrénées, 14 Av. E. Belin, 31500 Toulouse, France. E-mail: stephane.calmant@cnes.fr

M.-N. BOUIN

ENSG/LAREG
Institut Géographique National
Marne la Vallée, France

A bottom pressure gauge (BPG) was installed in proximity (3.7 km at closest approach) of Jason-1 and formerly TOPEX/Poseidon (T/P) ground track No. 238 at the Wusi site, located ~10 km offshore off the west coast of Santo Island, Vanuatu, Southwest (SW) Pacific. Sea level variations are inferred from the bottom pressure, seawater temperature, and salinity, corrected for the measured surface atmospheric pressure. The expansion of the water column (steric increase in sea surface height, SSH) due to temperature and salinity changes is approximated by the equation of state. We compare time series of SSH derived from T/P Side B altimeter Geophysical Data Records (GDR) and Jason-1 Interim Geophysical Data Records (IGDR), with the gauge-inferred sea level variations. Since altimeter SSH is a geocentric measurement, whereas the gauge-inferred observation is a relative sea level measurement, SSH comparison is conducted with the means of both series removed in this study. In addition, high-rate (1-Hz) bottom pressure implied wave heights ($H_{1/3}$) are compared with the significant wave height (SWH) measured by Jason-1. Noticeable discrepancy is found in this comparison for high waves, however the differences do not contribute significantly to the difference in sea level variations observed between the altimeter and the pressure gauge. In situ atmospheric pressure measurements are also used to verify the inverse barometer (IB) and the dry troposphere corrections (DTC) used in the Jason IGDR. We observe a bias between the IGDR corrections and those derived from the local sensors. Standard deviations of the sea level differences between T/P and BPG is 52 mm and is 48 mm between Jason and BPG, indicating that both altimeters have similar performance at the Wusi site and that it is feasible to conduct long-term monitoring of altimetry at such a site.

Keywords bottom pressure gauge, Jason, satellite altimetry, sea level, verification

The MOTEVAS project (*Mouvements Océaniques et TEctoniques Verticaux par Altimétrie Spatiale*, or Oceanic and TEctonic Vertical Movements by Space Altimetry, in English), is primarily dedicated to measure crustal motion in the oceanic domain using multiple datasets, including pressure measured by bottom pressure gauges (BPG) and sea surface height (SSH) changes provided by satellite altimetry. The project area is near the west coast of Santo Island, Vanuatu, South West Pacific (Figure 1). There, the Australia plate subducts beneath the Vanuatu archipelago along the New Hebrides trench. Because the Australia plate bears the D'Entrecasteaux aseismic ridges that resist subduction, this site is located in a region of active tectonics (Calmant et al. 2003a), including occurrence of large earthquakes. In the frame of this project, two BPG-Seabird 26 wave and tide recorders are currently operating at the Wusi and Sabine banks (see location on Figure 1) since November 1999 and are used in this study.

The Wusi gauge is immerged under the Jason-1 descending track No. 238, and is about 10 km away from the west coast of Santo Island. Gauge depth is about 12 m. The Sabine gauge is immerged on Sabine Bank, shallow top of one of the seamounts making the D'Entrecasteaux Ridge. Its depth is about 15 m. Both gauges are mounted in steel frames anchored into coral flats. The gauge data are retrieved by divers once a year, and the gauges are removed every other year for instrumental calibration. In addition to the pressure, seawater temperature and salinity are recorded at both gauges.

The sea level variation with respect to the time-averaged mean sea surface can be inferred from the bottom pressure, directly measured by a BPG, corrected using auxiliary

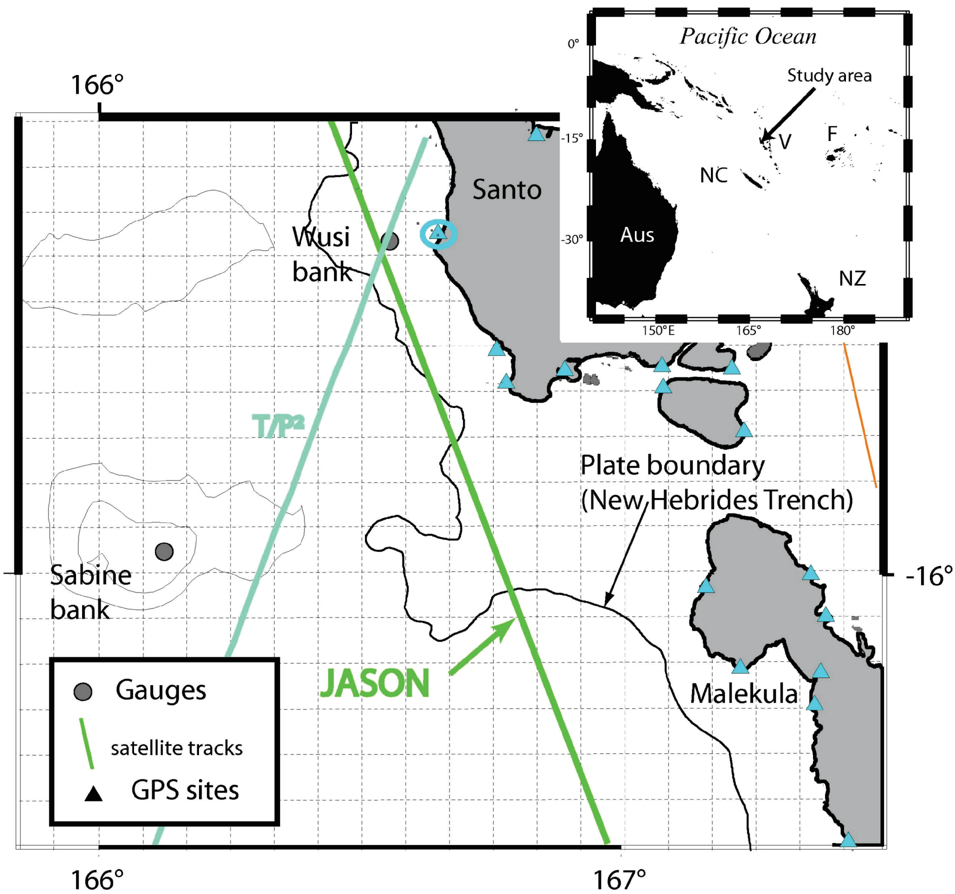

FIGURE 1 Map of the MOTEVAS project area in South Pacific. Track 238 of satellite Jason-1 and TOPEX primary mission and Track 199 of T/P new orbit starting on August 15, 2002 after the orbit maneuver are shown, with 1-km width. Locations in the upper right inset: Aus: Australia; NC: New Caledonia; V: Vanuatu and F: Fiji.

measurements such as water temperature and salinity and surface atmospheric pressure. The bottom pressure is not sensitive to steric effects caused by the volume expansion of the water due to changes of temperature and salinity. Since one of the goals of this study is to compare the sea levels inferred from BPG and altimeter SSH measurements, the contribution of the thermo-haline steric effects must be accounted for. Hence, the equation of state (Leendertse and Liu 1978), which provides a functional relationship between the seawater density, temperature, and salinity, is used in this study to account for thermosteric and halosteric effects. Second order thermo-haline effects that are not fully quantified in the equation of state are ignored in this study. A test is conducted empirically with the bottom and surface atmospheric pressures, seawater temperature and salinity to quantify the effects in the inferred sea level contributed by the changes of pressure and of the seawater density. The details are discussed in the next section.

The sea level comparison in this study is done in the relative sense. The altimeter SSH is geocentric and refers to a specified reference ellipsoid, whereas the gauge-inferred sea level is a relative measurement. Hence, no absolute SSH comparison is attempted in this study. The mean in both altimeter SSH series as well as in the gauge-inferred sea level is removed. The SSH difference or sea level difference defined henceforth is the height difference between the mean-removed time series from altimeter SSH and from the BPG sea level. The future work of this project includes the deployment of a Global Positioning System (GPS) equipped vessel over the BPG. It will connect the gauge-inferred sea level to the geocentric height, which will allow absolute comparison with altimeter SSH. In addition, the Wusi and Sabine gauges are located on different plates and thus allow us to analyze the relative vertical movement by cross referencing both datasets.

TOPEX/Poseidon (T/P) is a joint radar altimeter satellite mission by National Aeronautics and Space Administration (NASA), USA, and Centre National d'Etudes Spatiales (CNES), France. The spacecraft was launched on 10 August 1992. The near-circular T/P orbit is designed to repeat every 10 sidereal days, with a 66° inclination and an altitude of 1354 km (Fu et al. 1994). The TOPEX altimeter has redundant Sides A and B hardware. Data from Side A began to show performance degradation six years after launch. The TOPEX Science Working Team decided to switch to the Side B altimeter at 15:04 UTC on 10 February 1999 for future operation (TOPEX Team 2000). The CNES/NASA mission Jason-1 was launched on 7 December 2001 with an identical orbit as T/P. During its first month of operation, Jason-1 was placed in tandem with T/P for instrument calibration, and it is shown that its performance is similar to T/P. Since 15 August 2002, T/P was moved to a new orbit (one track is close to the MOTEVAS project area, see Figure 1), with ground-tracks half-way between its original orbit tracks providing a double space-time sampling with Jason-1 (Menard et al. 2003).

Sea Level Inferred from Bottom Pressure Gauge Data

The ocean bottom pressure measured by the BPG is an integral of water density as a function of depth, increased by the sea surface atmospheric pressure. The hydrostatic relation (Park and Saint-Guily 1992) is used to correspond pressure, density, and seawater column above the BPG:

$$P_b - P_a = g \int_{-h}^{0} \rho(z) dz, \tag{1}$$

where P_b is the bottom pressure measured by the gauge, P_a is the atmospheric pressure at the sea surface, g is gravity, ρ is seawater density and z is the vertical axis pointing upward with 0 and $-h$ indicating the mean sea surface and gauge depth, respectively. The height of the water column, h, derived from the bottom pressure using Eq. (1) does not include the steric component of the sea level because steric effect causes volume expansion without changing the pressure, unless thermo-haline contributions are also considered in the density variations. Hence, the steric (thermal and salinity) effect is considered using the equation of state (Leendertse and Liu 1978), as shown in Eq. (2). It provides the seawater density as a function of temperature and salinity:

$$\begin{aligned} \rho(z) &= \rho(T, S) \cong 10^3 \frac{P_0}{A_1 + 0.698 P_0}, \\ P_0 &= 5890 + 38T - 0.375T^2 + 3S, \quad \text{and} \\ A_1 &= 1779.5 + 11.25T - 0.0745T^2 - S(3.8 + 0.01T), \end{aligned} \tag{2}$$

where temperature T is in °C and salinity S is in practical salinity unit (psu).

Since we have temperature and salinity measurements at the depth of the gauge only, we assume that the sea temperature and salinity are constant in the seawater column above the gauge, and that density variations are related only to the time variations of the temperature and salinity based on the equation of state. Although the gauges are located in shallow water (12–15 m deep), this assumption may introduce a small error in the computation of the height of water column above the BPG. Hence, the height of the total water column above the gauge (including the steric effect) is obtained by rearranging Eq. (1) with the water density derived from Eq. (2) using the real temperature and salinity measurements.

$$h = \frac{P_b - P_a}{g \cdot \rho(T, S)}. \tag{3}$$

Then the mean column height is removed to determine SSH variation. Substituting the bottom and atmospheric pressure data and assuming the water temperature changes from 4° to 30°C with 35 psu salinity, it is found that the steric effect contributed to sea level change for about 8 cm. This is in excellent agreement with the SSH variation caused by the thermal effect (6 cm) estimated by using the World Ocean Atlas 2001 (WOA01) at 15.5°S and 165.5°E (National Oceanographic Data Center 2003; Martinez-Benjamin et al. 2004).

The BPG collect bottom pressure data every second and an average pressure is recorded internally every 15 minutes. Four minutes of the 1 Hz pressure data is also saved internally every 3 hours. The latter data are further used to derive wave heights. The device that we installed on land at Wusi village to record the atmospheric pressure suffered technical problems and the data used in this study exhibited significant periods of data gaps. We thus filled the data gaps using measurements recorded by the station operated by the National Tidal Facility at Port-Vila, about 200 km south of Wusi. Analysis of both datasets for overlapping sequences showed that the measurements at Port-Vila provide a satisfying proxy for that at Wusi. However, short wavelength phenomena such as the pressure drop related to cyclones cannot be recorded accurately with such a separation of distance. A mean pressure bias of 3.2 mbar found between the two time series has been removed from the Wusi measurements to fit the Port-Vila series, which are referenced to sea level.

The pressure gauge anchored on the seafloor at the Wusi site experienced a 37 mm uplift related to the earthquake that occurred beneath Santo Island at 20:48 UTC on 4 October 2000. The gauge at Sabine did not undergo noticeable coseismic motion, given its location on the Australia plate, at the rear of the subduction trench. The 37 mm have been determined in order that the series of mean sea level (tides being filtered out by a 3-day filter) present the same trend at both gauges. It is in close agreement with the 54 ± 11 cm offset found by GPS on land (Calmant, unpublished data), a few kilometers eastwards. This uplift of 37 mm from 4 October 2000 is applied to the Wusi gauge series used further in this study. Differences between the mean sea levels (tides being removed by a 3-day filter) recorded at both gauges are presented in Figure 2. Slope of the trend fitting these differences is zero by removing the coseismic jump of 37 mm at Wusi. The standard deviation is 30 mm. The scatter of this sea level difference is likely due to spatial and temporal atmospheric pressure variations and currents, which are not taken into account in this study.

Sea Surface Heights Inferred from Satellite Radar Altimeter Data

Satellite radar altimeters emit and receive radar pulses and measure their travel time when they are bounced back from the water surface on the earth. One of the primary observables of radar altimeter is the SSH:

$$\text{SSH} = a - d\text{-corrections}, \tag{4}$$

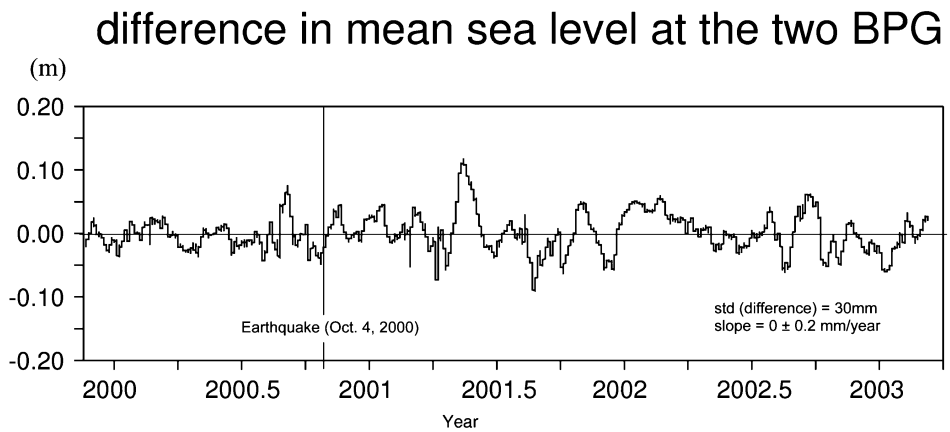

FIGURE 2 Mean sea level differences (3-day filter applied for tides) between Wusi and Sabine BPG. The time series at Wusi had been corrected for the 37 mm uplift caused by the earthquake on 4 October 2000.

where a is the altimeter orbital height above the reference ellipsoid computed using a precision orbit determination procedure, d is the range measurement computed from half of the travel time of the radar pulse and the speed of light. There are typically three categories of corrections on altimetric data: the instrument, media, and geophysical corrections. The instrument corrections are due to the variations in spacecraft hardware resulting from the nature of the return signal, satellite motion and pointing errors, satellite temperature variations, and other hardware properties. They include, among others, Doppler corrections, center-of-mass offsets, mispointing tracking adjustments, and internal and sea state bias (SSB) corrections. The media corrections are associated with the delay of the radar signal by the atmosphere, including the ionosphere delay, and dry and wet troposphere delays. The geophysical corrections include tides (solid Earth tide, ocean tide, and pole tide) and the inverse barometer (IB) correction.

Since altimeter SSH measurements are to be compared with the BPG sea level data, the ocean tide and the IB corrections are not applied to the altimeter SSH because the gauge-inferred sea level contains tidal and atmospheric pressure signals. Due to the repeat orbit design, the altimeter footprints are scattered within a small (± 1 km along the orbital groundtrack) geographical region. Figure 3 shows a typical Jason-1 repeat groundtrack (No. 238) near the Wusi gauge. The 1-Hz footprints scatter approximately in a 2- by 6-km area in the cross- and along-track directions. High rate altimeter data records (orbit and range) are available (i.e., 10 Hz for T/P; 20 Hz for Jason-1) from the Geophysical Data Records (GDR) for T/P or the Interim GDR (IGDR) for Jason-1 and the 1-Hz SSH is computed by subtracting the averaged high-rate range from the averaged high-rate orbit. Since the Wusi gauge is not exactly located on these T/P and Jason-1 tracks, a correction of the geoid gradient from the gauge site to the corresponding 1-Hz altimeter footprint is required. The mean sea surface model CLS01 with a regular grid of $2'$ by $2'$ (Hernandez and Schaeffer 2001) is used in this study to account for the gradient difference between the altimeter and the gauge locations.

Sea level comparisons are conducted for each of the altimeter passes over the BPG. The corresponding gauge sea level data are filtered by an order three polynomial within a one-hour bottom pressure data span. As mentioned before, the SSH comparison is made in the relative sense with their means removed. The scattering of the SSH difference around the mean, or the standard deviation, is computed. The drift is estimated using a linear model

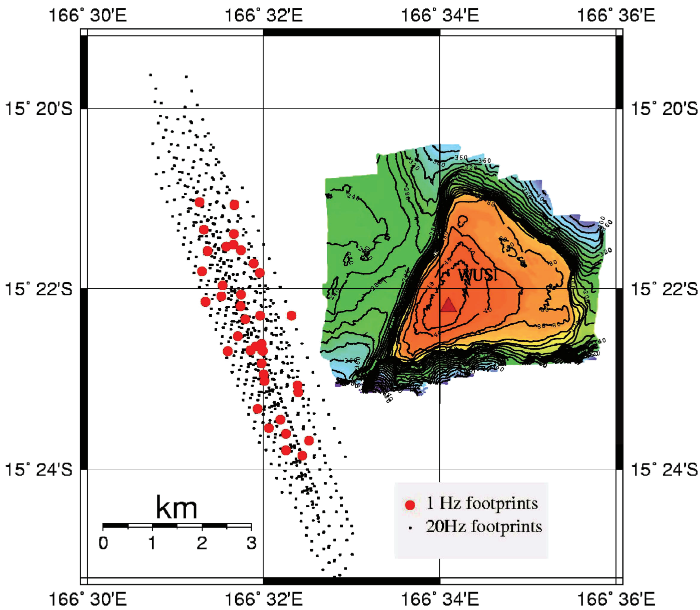

FIGURE 3 Jason-1 altimeter footprint locations near the Wusi gauge. The 1-Hz footprint location represents the average location of the consecutive valid high-rate data (20 Hz) in each cycle. Triangle stands for the location of the gauge. The bathymetric contour interval is 20 m.

from these mean-removed SSH differences. The estimated drift (with adequate data span) represents the overall time-varying effect of the differenced sea level, including instrumental effects, drifts from various corrections and crustal movement at the BPG.

TOPEX/Poseidon Side B Sea Surface Height Data

In this study, we used the GDR released from Archiving, Validation and Interpretation of Satellite Oceanographic data (AVISO). They are the global along-track altimeter measurements averaged every 1 second with all corrections applied. The Merged GDR (MGDR) are generated from TOPEX and Poseidon measurements to reinforce unity of the T/P mission (AVISO 1996). The T/P dataset used in this study is part of the Side B data (from Cycles 264 to 363). The applied corrections and the data editing criteria can be found in AVISO (1996). The time span of these cycles is from December 1999 to July 2002. For comparison with the gauge-inferred sea levels, the ocean tides and the IB corrections, which have been applied to the MGDR, have to be added back.

Jason-1 Sea Surface Height Data

The Interim GDR (IGDR) released from AVISO for Jason-1 are used in this study. Some of the corrections in Jason-1 IGDR have been updated and are not identical to corrections in T/P GDR. The list of corrections and the data editing criteria can be found in CNES and JPL (2003). Jason-1 IGDR used in this study are from Cycles 2 to 43 that are from February 2002 through March 2003. Similar to what has been done to T/P, the ocean tides and the IB corrections are added back to the IGDR SSH product since the gauge-inferred sea levels contain both signals.

CNES and JPL (2003) state that the accuracy of the SSB models remains limited and continues to be a topic of research. Hence we tested different SSB models for the use of Jason-1 SSH products including: (1) the SSB model from the IGDR, which is a bilinear interpolation of a table of sea state biases versus significant wave height and wind speed, based on nonparametric fits by Gaspar et al. (1994) with the data from Cycles 19–30 of the Jason-1 mission, (2) the 4-parametric SSB model by Chambers et al. (2003a), and (3) the nonparametric model by Gaspar et al. (2002), which has been adopted for production of future Jason-1 GDR (Chambers et al. 2003b). These models are designated as SSB_IGDR, SSB_4PAR, and SSB_CLS in this study.

Results

Sea Level Comparison of T/P and BPG

T/P footprints scatter near the Wusi site as do the Jason-1 footprints (Figure 3). To limit the effect of the along track geoid gradient, 10 high-rate (10 Hz) valid T/P footprints in each cycle are selected centered at latitude 15.7°S and their averaged SSH are calculated. The comparison with the gauge-inferred sea level measurements is then made with the derived average, instead of the original 1-Hz T/P SSH. Cross-track gradients are accounted for using the CLS01 mean sea level model.

The sea level differences between T/P and BPG are shown in Figure 4. Standard deviations for the different cases are summarized in Table 1. We note that accounting for

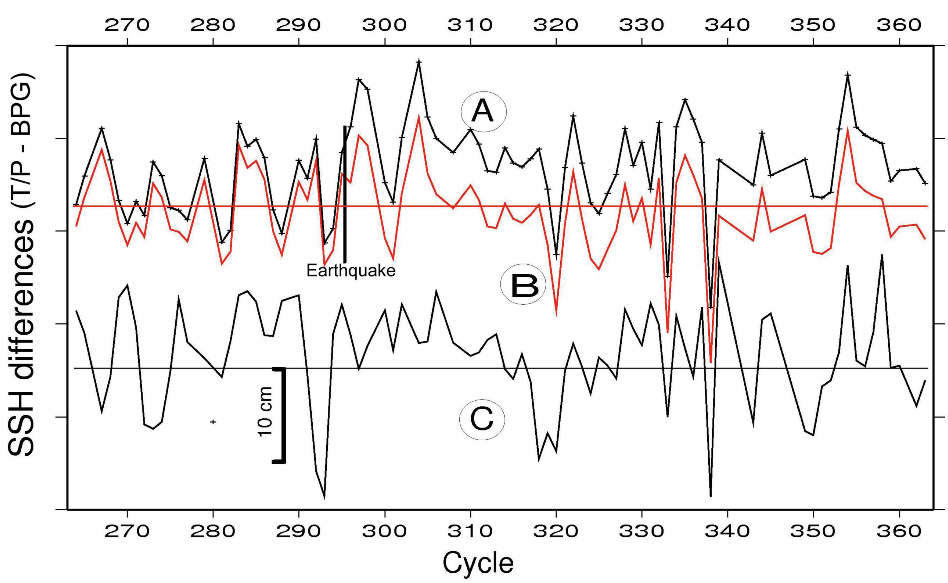

FIGURE 4 Series A: the difference between T/P Track No. 238 SSH and the inferred sea levels at the Wusi gauge. Ten high-rate T/P SSH are combined at 15.7°S latitude. Series B (in gray): same as A with 37 mm earthquake-related uplift corrected in the sea levels inferred at the Wusi gauge. Series C: the difference between T/P Track No. 238 and the sea levels inferred at the Sabine gauge. Ten high-rate T/P SSH are combined at 16°S latitude. Combination of high-rate SSH is to remove the along-track gradient, whereas the cross-track gradients are corrected with CLS01 mean sea surface model. The start and stop time of the series are 1999/12/03 and 2002/07/31.

TABLE 1 Drift Estimates and Standard Deviations of SSH Differences Between T/P SSH Track No. 238 and BPG Series

Series in Figure 4	T/P–BPG (Wusi) Series A (Earthquake displacement not corrected)	T/P–BPG (Wusi) Series B (Earthquake displacement corrected)	T/P–BPG (Sabine) Series C
Drift (mm/year)	16.6 ± 8	-1.6 ± 8	-0.9 ± 9
Std Dev. (mm)	55	52	62

the coseismic step in 4 October 2000 reduces both the slope and standard deviation of the residuals between the T/P-derived and Wusi BPG-derived SSH series. The scatter is significantly larger in Series C, computed using Sabine bank SSH series. The gauge-inferred sea levels from both gauges agree well with a standard deviation of 30 mm when tides are filtered out (Figure 2). Hence, the increase in the standard deviation in Series C compared to Series B is due to a spatial distance increase, which can be related to high-frequency atmospheric pressure changes, tide residuals, internal tides and currents. In addition, the drift estimates are the combined effect of altimeter drift from the instruments and from the corrections, BPG instrument and the secular part of its vertical movement.

Sea Level Comparison of Jason-1 and BPG

SSB Model Comparison of Jason-1 and BPG

The Jason-1 SSH series with the use of three different SSB models are compared to the sea levels inferred at the Wusi gauge. The mean-removed height difference between them is computed and the standard deviation of the height differences and a drift estimate are calculated. Table 2 summarizes the result. It is clear that all models improve the fit between Jason-1 SSH to the BPG since the highest standard deviation is found when no SSB model is applied. Moreover, when SSB_CLS model is applied to Jason-1 SSH time series, it has the smallest standard deviation at 48 mm. This indicates that the application of SSB_CLS model to Jason-1 SSH gives better results (for Cycles 2 to 43 used in this study) when compared with the sea levels inferred at the Wusi gauge than the other two models do. Hence, the CLS model was chosen to be applied to the Jason-1 SSH for the analyses in the next session. A direct comparison between Jason-1 SSH with different SSB models is made in Figure 5. A 5-cm bias from the CLS model to the other two models is evident.

Sea Surface Height Comparison of Jason-1 and BPG

Since the high-rate (20 Hz) Jason-1 does not include all corrections properly (B. Beckley, personal communication, 2003), only 1-Hz IGDR SSH product of Jason-1 is

TABLE 2 The Comparison of Jason-1 SSH (Cycle 2–43, 2002/02/03–2003/03/16) with the Use of Different SSB Models to the Sea Levels Inferred at the Wusi Gauge

	No SSB	SSB_IGDR	SSB_4PAR	SSB_CLS
Drift estimate (mm/year)	-56.2 ± 26	-55.7 ± 22	-55.5 ± 22	-47.6 ± 20
Std Dev. (mm)	62	53	51	48

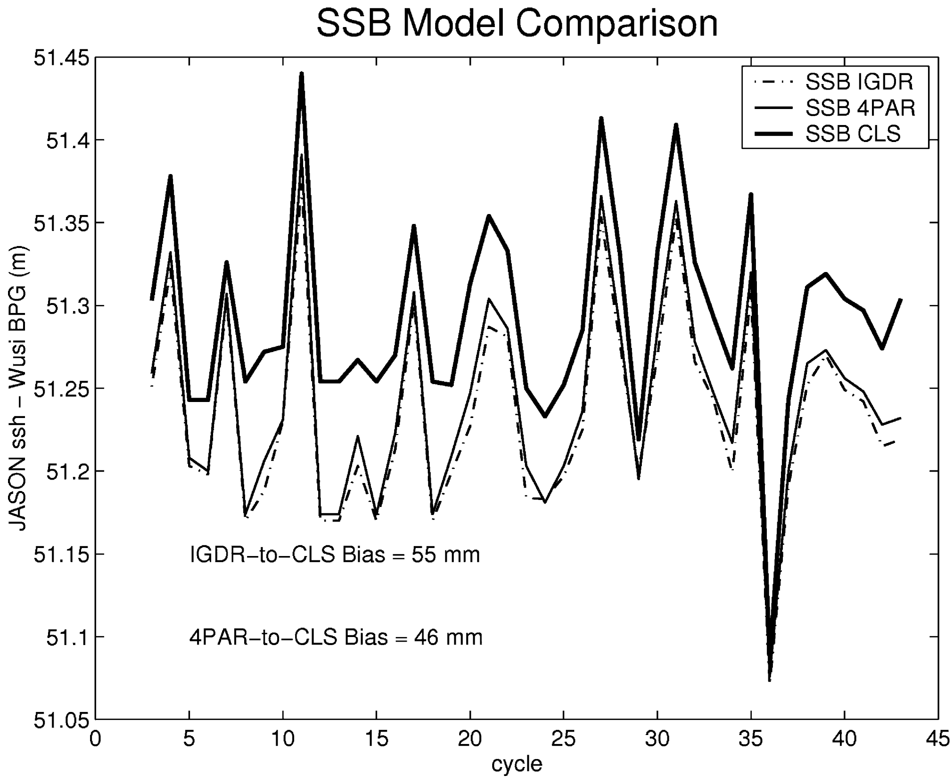

FIGURE 5 Jason-1 SSH series (Cycles 2–43; 2002/02/03–2003/03/16) with different SSB models applied.

used in the comparison. The standard deviation of the height differences between Jason-1 SSH and the sea levels inferred from the Wusi gauge is computed. A drift representing the overall time-varying effect in each scenario is calculated. Different scenarios were selected; results are summarized in Table 3. Clearly, the first scenario (shown in Figure 6) with smallest standard deviation shows the best coherence between the Jason-1 SSH and the gauge-inferred sea level with means removed. The solid Earth tide, wet troposphere, and the gradient corrections are more significant compared to other corrections. The drift estimates are significantly different since it represents the drift from each individual correction being analyzed in each scenario. Yet, the uncertainties associated with these drifts are large, suggesting that longer series are required before definite conclusions can be drawn on the meaning of these drifts.

A study has been conducted using the University of Texas CSR orbit in place of the CNES orbit, which is originally provided from the IGDR. It is found that the change of the orbit does not significantly change the standard deviation of height difference (50 mm for CSR orbit; 48 mm for CNES orbit).

Analysis of the Significant Wave Height

The pressure gauge we used, Seabird 26, is designed not only for tide recording but also for wave height monitoring. As mentioned before, 240 1-Hz bottom pressure readings are recorded at the gauge every 3 hours. These high frequency pressure readings were converted to $H_{1/3}$ using the manufacturer's software package (www.seabird.com/product/spec_sheet/

TABLE 3 Results of the Jason-1 and Wusi Gauge Sea Level Comparisons, with Different Choices of Corrections or Orbits

Drift estimate (mm/year)	Std Dev. (mm) in height difference	Selected SSB model	Selected Orbit	Scenarios
-48 ± 20	48	SSB_CLS	CNES	Apply load tide, pole tide, solid Earth tide, dry/wet troposphere and ionosphere corrections. CLS01 mean sea surface model is used to provide the gradient corrections.
-44 ± 21	48	SSB_CLS	CNES	Pole tide correction not applied.
-35 ± 21	50	SSB_CLS	CNES	Load tide correction not applied.
-49 ± 20	50	SSB_CLS	CSR	Substitute IGDR orbit with CSR orbit.
-46 ± 21	50	SSB_CLS	CNES	Dry troposphere correction not applied.
-56 ± 22	51	SSB_4PAR	CNES	Substitute SSB_CLS with SSB_4PAR.
-56 ± 22	53	SSB_IGDR	CNES	Substitute SSB_CLS with SSB_IGDR.
-56 ± 26	62	—	CNES	SSB model not applied.
-13 ± 32	71	SSB_CLS	CNES	Ionosphere correction not applied.
-14 ± 41	88	SSB_CLS	CNES	Wet troposphere correction not applied.
73 ± 46	110	SSB_CLS	CNES	Gradient (CLS01) not applied.
49 ± 63	138	SSB_CLS	CNES	Solid Earth tide correction not applied.

26plusdata.htm). Then we compare Jason-1 significant wave height (SWH) from the IGDR to these gauge-inferred wave heights ($H_{1/3}$). Figure 7 shows the comparison of the SWH and the corresponding gauge-inferred wave heights as a function of 10-day Cycle numbers. The gray scale represents the mean-removed sea level differences. Figure 7 reveals that Jason-1 SWH is consistent with the gauge-inferred wave height for small waves (height less than 3 m). The slope of the best-fit regression line, expressed as a thick line in Figure 7, is 0.66 ± 0.14 for small gauge-inferred waves. The slope does not indicate a strong correlation between these two time series. For larger wave heights, between 3 and 6 m, altimeter SWH measurements are different and vary from 1.5 to 3.5 m.

In addition, we analyzed the relationship between SSH difference and the wave difference (between SWH and the gauge-inferred waves) but no clear correlation is evident. In conclusion, the Jason-1 IGDR SWH for Cycles 2 to 43 are not fully consistent with the wave heights determined from the 1-Hz bottom pressure recorded in situ by the gauge. Larger discrepancies occur for wave heights between 3 and 6 m. Further investigation with longer datasets or additional observations using other devices, such as the GPS buoy/vessel, are necessary.

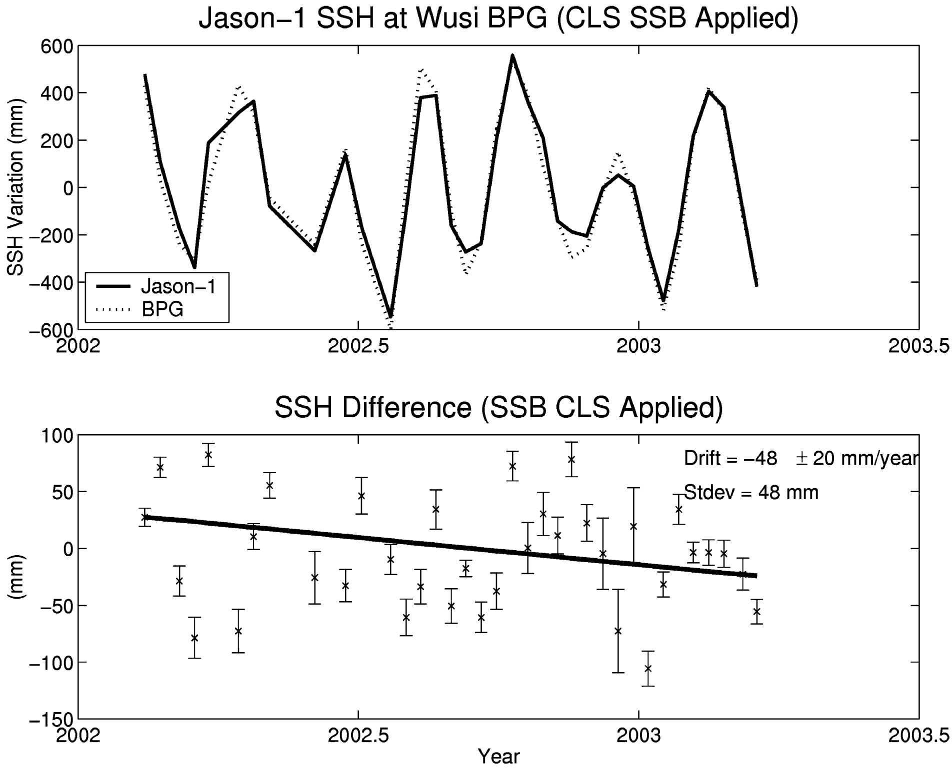

FIGURE 6 (Top) Jason-1 SSH and the sea levels inferred at the Wusi gauge. Both means have been removed. (Bottom) Height differences and associated uncertainties are shown. The Jason-1 data are from cycles 2 to 43 (2002/02/03–2003/03/16). The corrections applied to Jason-1 SSH are: load tide, pole tide, solid Earth tide, dry/wet troposphere and ionosphere corrections. CLS01 mean sea surface model is used to correct the Jason-1 SSH for the geoid gradient. CNES orbit provided by IGDR is used.

Analysis of Air Pressure Effects

Dry Troposphere Correction (DTC) directly depends on atmospheric pressure. At 15°S, this correction is described in Eq. (5), where P_{atm} is the instantaneous atmospheric pressure (CNES and JPL, 2003).

$$\text{DTC(mm)} = -2.2821 \cdot P_{\text{atm}}(\text{mbar}). \tag{5}$$

The IGDR DTC variations are well correlated to the in situ values determined by merging local atmospheric pressure measurements from nearby sensors using Eq. (5). The correlation between both series is 0.91 as shown in Figure 8 top panel.

Yet, a clear 41 mm bias is observed between both series, equivalent to a 18 mbar offset. The IGDR DTC are unusually small since they range between −2.276 m and −2.248 m, which turn to pressure ranging between 997 mbar and 985 mbar. Such low pressure values are not recorded either at the Wusi pressure sensor or at the Port-Vila tide gauge (both are merged to form the local series reported in Figures 8 and 9) nor at the Pekoa airport (50 km East of Wusi). This large offset cannot be explained by some misreferencing to sea level, of the local sensors, since it would imply that the three sensors are below sea

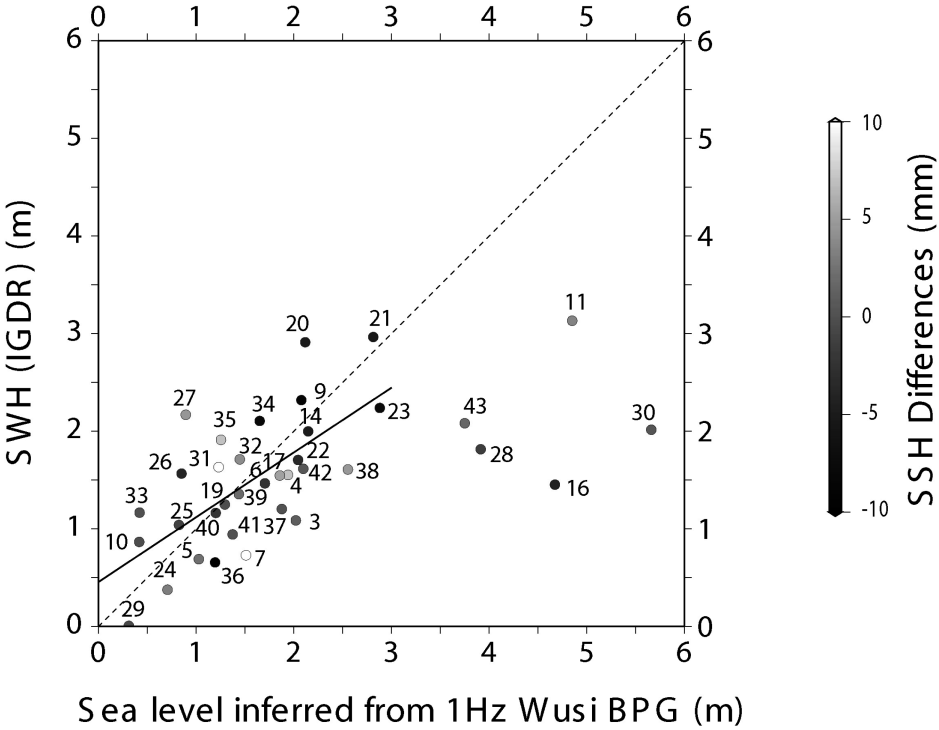

FIGURE 7 Comparison of SWH in Jason-1 IGDR (Cycles 2–43; 2002/02/03–2003/03/16) to the sea levels inferred from the 1-Hz bottom pressure readings at the Wusi gauge. The SWH-to-gauge comparison at each cycle is labeled with the cycle number and its gray code represents the mean-removed SSH difference between Jason-1 SSH and the gauge-inferred sea levels. The thick line stands for the best fitting regression line when the inferred wave height is less than 3.0 m. The dotted line stands for perfect and unbiased agreement (slope = 1).

level, given that they present higher pressure values than the IGDR DTC, or that unrealistic calibration errors affect all three sensors. It is worth noting that typical errors of 10 mbar may occur in the South Pacific Ocean, as stated in the Jason-1 User Handbook (CNES and JPL, 2003). Further study with longer series and careful analysis of the ECMWF fields (European Center for Medium Range Weather Forecast) data that are used to derive the IGDR DTC are required to fully understand this bias. Yet, this area is particularly under-sampled, and it is a place where extreme short time and space variations of the atmospheric pressure are common. This may have affected the large-scale average values in the ECMWF fields.

It is also worth noting that the differences in DTC (bias removed) are not correlated to the SSH differences (correlation is 0.06, lower panel of Figure 8). Thus the former does not participate significantly to the scatter in the SSH differences.

Although the IB correction is not used in the present study, we present an analysis of the accuracy of the IB correction from ECMWF packed in the IGDR by comparing it with ground-truth values recorded on land, at the Wusi village, ~10 km east of the Wusi gauge. The IB effect in terms of sea level is:

$$IB = -9.948(P_{atm} - P), \quad (6)$$

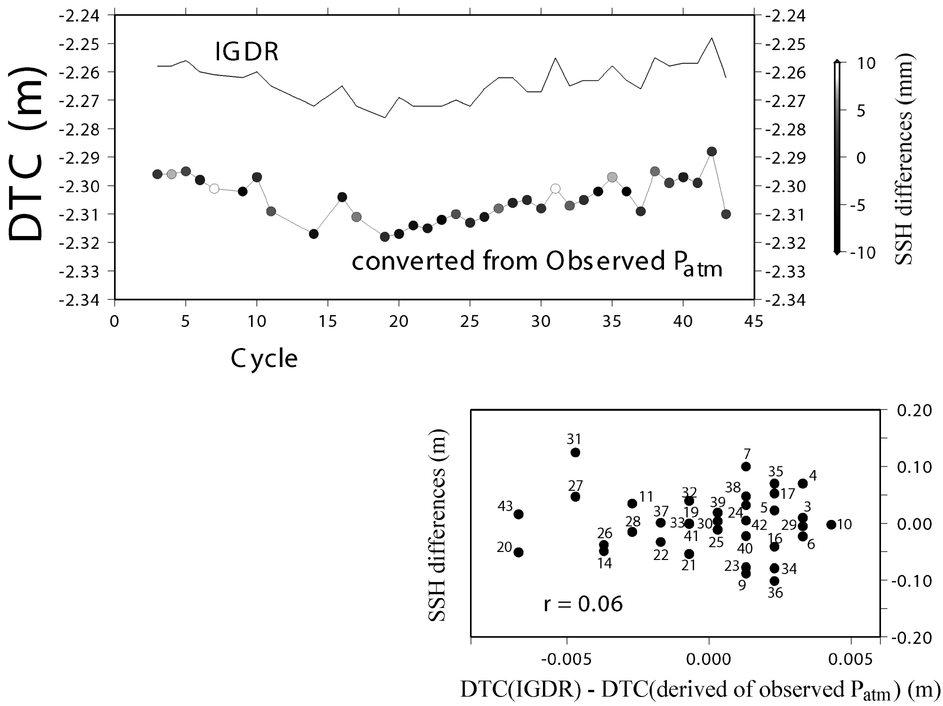

FIGURE 8 (Top) Effect of atmospheric pressure estimates on the Dry Tropospheric Correction. Gray code of the dots stands for the mean-removed SSH difference between Jason-1 and the gauge-inferred sea level. The Jason-1 data are from cycles 2 to 43 (2002/02/03–2003/03/16). A clear 41 mm bias can be seen. (bottom) Relationship between the SSH difference and the difference in DTC in relative sense. The two datasets are poorly correlated (correlation is 0.06).

where IB is in mm, P_{atm} is the instantaneous atmospheric pressure, and P is the long-term mean of the global surface atmospheric pressure over the oceans (CNES and JPL 2003). The scale factor -9.948 mm/mbar is an empirical value for mid latitude (Wunsch 1972).

The mean global surface atmospheric pressure over the oceans is 1010.9 ± 0.6 mbar, using ECMWF pressure values obtained during the first eight years of the T/P mission. However, T/P products provide the IB correction with P being a constant, 1013.3 mbar (CNES and JPL 2003). Given the questioning on the ECMWF reference pressure mentioned before, we adopted this value of 1013.3 mbar as P in Eq. (6) with the ground-truth records at Wusi village to verify IB correction from Jason-1 IGDR. The result is shown in Figure 9. The mean values of both datasets (188.65 mm in Jason-1 and 9.46 mm in the ground-truth records) are removed. The slope of the linear fit between both IB series is estimated to be 0.82 ± 0.05, and both datasets are well correlated (with 0.91 correlation). The discrepancies in these two datasets are likely caused by the fact that Jason-1 IB correction is derived from a worldwide, large-scale pressure model such as ECMWF that does not fully represent the atmospheric variations at short scale in space and time as in this study. In addition, choosing a single mean atmospheric pressure, 1013.3 mbar, as well as the scale factor -9.948 in Eq. (6), also in part cause discrepancies in both series.

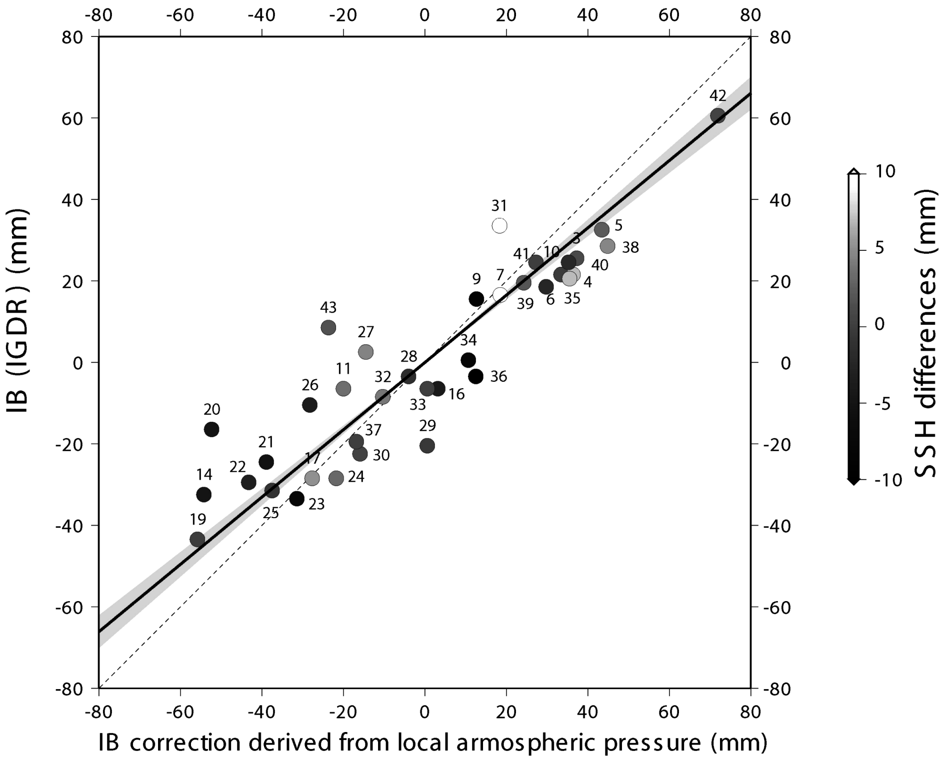

FIGURE 9 Relative comparison between IGDR IB correction and the IB correction computed based on in situ records of the atmospheric pressure. The means of both have been removed. The global time-varying mean atmospheric pressure over the oceans is selected to be 1013.3 mbar. The Jason-1 data are from cycles 2 to 43 (2002/02/03–2003/03/16). The cycle number is labeled with each comparison. The thick line stands for best fitting regression line and the associated gray band stands for the uncertainty on the slope. Gray code of the dots stands for the mean-removed SSH difference between Jason-1 SSH and the gauge-inferred sea levels. The dotted line stands for perfect agreement (slope = 1).

Conclusions

The use of a BPG and auxiliary measurements such as water salinity and temperature and surface atmospheric pressure to infer the sea level variations with respect to the mean sea surface is discussed in this article. The SSH variation caused by the steric expansion due to the thermo-haline steric effects of the seawater are approximated with the equation of state in terms of the seawater density. A small error might result from the assumption that the water density does not vary with depth above the gauge (about 12–15 m deep) at a given time since no vertical profile of the water column density is available. However, the steric effect at the Wusi gauge approximated in the present study is comparable to that estimated by WOA01 model at the closest grid node (15.5°S, 165.5°E).

The difference in SSH from the Wusi gauge data and the T/P data shows a standard deviation of 52 mm, whereas the difference with the Jason-1 SSH presents a 48 mm standard deviation. In these comparisons, the ocean tide and the IB corrections are added back to the altimeter SSH obtained from the altimeter GDR, since the contributions of ocean tides and atmospheric pressure are included in the gauge-inferred sea level. We conclude that T/P and Jason-1 sea level measurements perform similarly at the Wusi gauge, thus verifying the performance of both altimeter systems in a relative comparison.

The solid Earth tide correction, geoid gradient, and the wet troposphere correction, if not applied, cause significant change in the standard deviation of the sea level comparisons between Jason-1 altimeter and the BPG. The along-track gradient in T/P is avoided using high-rate (10 Hz) data and the cross-track gradient is corrected with CLS01 mean sea surface model. In the case of Jason-1, both gradients are corrected with CLS01, since the valid high-rate (20 Hz) SSH were unavailable at the time of processing. Nevertheless, an accurate local geoid model is desirable for the gradient correction. The drifts estimated in T/P and in Jason-1 are significantly different. This is caused by the fact that the gradient correction in each case was treated differently and the datasets span different time windows. Longer series are necessary for the drift to be estimated more accurately.

The best coherence between Jason-1 and gauge sea level is found when the SSB_CLS model is used. However, the model has a 5-cm bias when compared with the other two models. The comparison for SWH shows a good agreement for waves smaller than 3 m, but we observe some disagreement for 3 m to 6 m inferred waves heights.

Comparisons of inverse barometer and dry tropospheric corrections with respect to ground-truth pressure observations show high correlation (0.91) in both cases. A 41 mm bias is found between the DTC series. The speculation for the disagreement includes that Jason-1 DTC are derived from a global large-scale model such as ECMWF, which does not contain the fine details of the pressure variation in such a short time and space scales. Also, the adopted time-varying mean of the global surface atmospheric pressure over the oceans, 1013.3 mbar, and the scale factor of −9.948 may participate in this discrepancy.

The new T/P orbit since August 2002 has a crossover point with the Jason-1 orbit in the vicinity of the Wusi BPG (Figure 1). That peculiar situation will enable an improved analysis of comparison between the two altimeters and the BPG measurements in the near future.

References

AVISO. 1996. *AVISO User Handbook: Merged TOPEX/Poseidon Products*. AVI-NT-02-101-CN, Edition 3.0.

Calmant, S., B. Pelletier, P. Lebellegard, M. Bevis, F. W. Taylor, and D. A. Phillips. 2003a. New insights on the tectonics along the New Hebrides subduction zone based on GPS results. *J. Geophys. Res.* 108(B6):2319–40.

Calmant, S., K. Cheng, and C. K. Shum. 2003b. Sea level series and GPS surveys along the ground track of satellite altimeters overflying the tide gauges of the MOTEVAS project. EGS-AGU-EUG Joint Assembly, April 6–11, Nice, France.

Calmant, S., T. Delcroix, A. Cazenave, and C. K. Shum. 2001. The Motevas project. *AVISO Altimetry Newsletter* 8:25–26.

Chambers, D. P., S. A. Hayer, J. C. Ries, and T. J. Urban. 2003a. New TOPEX sea state bias models and their effect on global mean sea level. *J. Geophys. Res.* 108(C10):3305–11.

Chambers, D. P., J. C. Ries, and T. J. Urban. 2003b. Calibration and verification for Jason using global along-track residuals with TOPEX. *Marine Geodesy* 26:305–17.

CNES and JPL. 2003. *AVISO and PODAAC User Handbook, IGDR and GDR Jason Product*, Ed. 2.0. SMM-MU-M5-OP-13184-CN (AVISO); JPL D-21352 (PODAAC).

Gaspar, P. S. Labroue, F. Ogor, G. Lafitte, L. Marchal, and M. Rafanel. 2002. Improving nonparametric estimates of the sea state bias in radar altimeter measurements of sea level. *J. Atmosph. Ocean. Tech.* 19:1690–1707.

Gaspar, P., F. Ogor, P. Y. Le Traon, and O. Z. Zanife. 1994. Estimating the sea state of the TOPEX and Poseidon altimeters from crossover differences. *J. Geophys. Res.* 99:24981–24994.

Gill, A. E., and P. P. Niller. 1973. The theory of the seasonal variability in the ocean. *Deep-Sea Res.* 20:141–177.

Fu, L. L., E. J. Christensin, C. A. Yamarone, M. Lefebvre, Y. Menard, M. Dorrer, and P. Escudier. 1994. TOPEX/Poseidon mission overview. *J. Geophys. Res.* 99(C12):24369–24381.

Hernandez, F., and P. Schaeffer. 2001. The CLS01 mean sea surface: A validation with the GSFC00 surface. Internal report CLS01_VALID_MSS.pdf, CLS Ramonville St Agne, France.

Leendertse, J., and S. Liu. 1978. A three-dimensional turbulent energy model for non- homogeneous estuaries and coastal sea systems. In *Hydrodynamics of estuaries and fjords*. J. Nihoul. (ed.). Elsevier, Amsterdam.

Martinez-Benjamin, J. J., Y. Yi, C. Kuo, A. Braun, Y. Chen, S.-C. Han, and C. K. Shum. 2004. GOCE data product verification in the Mediterranean Sea. Paper presented at Second International GOCE User Workshop, March 8–10, Esrin, Italy.

Menard, Y., L. L. Fu, P. Escudier, F. Parisot, J. Perbos, P. Vincent, S. Desai, B. Haines, and G. Kunstmann. 2003. The Jason mission. *Marine Geodesy* 26:131–46.

National Oceanographic Data Center. 2003. Datasets and products: World Ocean Atlas 2001. Available online at http://www.nodc.noaa.gov/OC5/WOA01/pr_woa01.html (Accessed May 1, 2004).

Park, Y., and B. Saint-Guily. 1992. Sea level variability in the Crozet-Kerguelen-Amsterdam area from bottom pressure and Geosat altimetry. In *Sea level changes: Determination and effects*, pp. 117–131. Geophysical Monograph 69, IUGG, Vol. 11.

TOPEX Team. 2000. *Special report, Side B testing status*. Available online at http://topex.wff.nasa.gov/sideb_status.html, NASA GSFC Wallop Flight Facility, Observational Science Branch, Wallops Flight Facility, Wallops Island, Virginia, USA.

Wunsch, C. 1972. Bermuda sea level in relation to tides, weather and baroclinic fluctuations. *Rev. Geophys. Phys.* 10:1–49.